Localization of Harmonic Source Using a Single Moving Sensor of Known Trajectory

Yi Yang Ang*+, Nam Nguyen+, Joni Polili Lie+, Woon Seng Gan*
*School of Electrical and Electronic Engineering, Nanyang Technological University, Singapore
+Halliburton Far East Pte Ltd, Singapore

***Abstract*—This paper presents a localization method for a harmonic source using a single moving sensor in a piecewise-linear trajectory with a known velocity. Through the movement of the sensor, spatial information is embedded in the recorded signal. An approach is proposed to extract that spatial information by reformulating the single-channel signal into multi-channel waveforms. A temporal correction factor is then derived and applied to approximate the multi-channel waveforms as the signals from multiple synthetic sensors to model a virtual static array. The proposed approach enables the construction of the array covariance matrix and applies a beamforming-based technique for source localization. Numerical results demonstrate that its statistical performance follows closely with the conventional sensor array approach. Finally, the paper also shows the experimental verification of the approach in a practical context of sound source localization using a single microphone.**

Keywords—sensor array, localization, single sensor, linear motion, synthetic aperture.

I. INTRODUCTION

Source localization is one of the key research subjects in array signal processing. Numerous approaches for a static array, such as the conventional delay and sum [1], correlation-based Capon [2], and subspace-based approaches, including MUSIC [3] and ESPRIT [4], have been derived based on the various signal and noise assumptions to obtain an optimal solution [5]. Although each of these algorithms has different strengths and weaknesses, all of them require multiple sensors to form an array for processing. The localization performance of the algorithms is directly proportional to the number of sensors used.

In recent years, a great deal of research has been conducted on extending the array apertures using moving sensor arrays [6]. These methods include the extended towed array measurement approach (ETAM) [7-9], which uses the correlation between the overlapping positions of each sensor to correct the mismatch attributable to its movement to form a larger synthetic array aperture. The moving circular array approach [10] has also been used, which requires a static sensor working in tandem with a rotating array. Still, few have considered the possibility of extending the array aperture with only a single sensor. Previously, Hioka and Kishida [11, 12] proposed the CAROUSEL architecture, which demonstrated that the directions of arrival (DOA) estimate could be achieved by using a single sensor moving along the circumference of a circle.

This paper shows that, if the trajectory of the sensor is either known or deduced from its known initial position and velocity, the piecewise-linear trajectory can be exploited to form a linear synthetic array aperture to localize a stationary source. The approach presented in this paper attempts to extend that of Hioka and Kishida by formulating the problem differently, such that it is not limited to the circular trajectory.

Section II first presents an introduction to the proposed method that considers only an acoustic monopole signal and the approach to reformulating the single channel into the multi-channel waveform. Next, the temporal correction factor is then derived from the multi-channel waveforms to extract the embedded spatial information and applied to approximate the recording as a virtual static array, the one sensor array (OSA). After the OSA is formed, localization can be achieved by solving it as a modified beamforming problem. Finally, the section ends with the extension of the OSA approach for monopole to a general harmonic source model. Section III includes numerical analyses conducted for monopole and harmonic sources. Section IV presents the experimental analysis to validate the proposed OSA approach on a set of experimental data collected with sensors mounted on an electric vehicle (EV). Section V presents the conclusions of the paper.

II. PROBLEM FORMULATION

A. Signal Model for Single Acoustic Monopole

Without loss of generality, consider a stationary point source signal captured by a single moving sensor as shown in Fig. 1. The source located at the spatial position $\boldsymbol{r}_s = (x_s, y_s)$ is denoted as:

$$s(t) = A_s e^{j(\omega t + \psi)}, \tag{1}$$

where $A_s, \omega,$ and ψ are the amplitude, angular frequency, and phase of the monopole, respectively. Because of the stationary assumption, A_s and ψ are assumed time-invariant.

This signal is recorded by the moving sensor $p(t)$, initially located at the origin $(x, y) = (0,0)$, and is expressed as:

$$p(t) = s(t)e^{-j\frac{\omega}{c}r(t)} + q(t), \;\; 0 \le t \le T, \tag{2}$$

where $r(t) = \|\boldsymbol{r}_s + \boldsymbol{v}t\|_2$ is the Euclidean distance between the source and sensor at time t moving with velocity $\boldsymbol{v}$; $q(t)$ is the additive white Gaussian noise used to model the spatial and

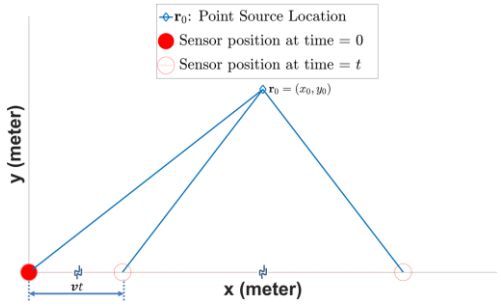

Fig. 1: Moving sensor configuration.

temporal noise inherent in the moving sensor. ω/c is the wavenumber of the source signal as the sensor moves within the recording window of T second. In addition, $e^{-j\omega r(t)/c}$ constitutes the phase shift because of the propagation of the signal toward the moving sensor. The collected samples can now be decomposed into N frames, such that each frame is quasi-stationary [13]. The nth frame can be expressed as:

$$p_n(t) = p(t + (n-1)\Delta T), \quad 0 \le t \le \Delta T\,, \tag{3}$$

where $\Delta T = T/N$ is the duration of each nth frame. The N frames can now be expressed in the vector form as:

$$\boldsymbol{p}(t) = [p_1(t) \quad \cdots \quad p_N(t)]^T, \quad 0 \le t \le \Delta T\,, \tag{4}$$

where $(.)^T$ denotes the transpose operation.

B. Design of Temporal Correction Factor

For brevity, $q(t)$ will be dropped from the signal model in (4), arriving at:

$$\boldsymbol{p}(t) = \begin{bmatrix} s(t + 0\,\Delta T)e^{-j\frac{\omega}{c}r(t+0\,\Delta T)} \\ \vdots \\ s(t + (N-1)\,\Delta T)e^{-j\frac{\omega}{c}r(t+(N-1)\,\Delta T)} \end{bmatrix}. \tag{5}$$

Rearranging (5) yields:

$$\boldsymbol{p}(t) = A_s e^{j(\omega t+\psi)} \underbrace{\begin{bmatrix} e^{j\omega\,0\,\Delta T} & 0 & 0 \\ 0 & \ddots & 0 \\ 0 & 0 & e^{j\omega\,(N-1)\,\Delta T} \end{bmatrix}}_{\text{Temporal Delay}} \underbrace{\begin{bmatrix} e^{-j\frac{\omega}{c}r(t+0\,\Delta T)} \\ \vdots \\ e^{-j\frac{\omega}{c}r(t+(N-1)\,\Delta T)} \end{bmatrix}}_{\text{Source Propagation}}, \tag{6}$$

Source Component

From (6), it is now clear that $\boldsymbol{p}(t)$ consists of a temporal-delay component, $e^{j\omega((n-1)\Delta T)}$, and its source with propagation component, $A_s e^{j(\omega t+\psi)-j\frac{\omega}{c}r(t+(n-1)\,\Delta T)}$. Here, two observations can be noted. First, if the nth $r(t + (n-1)\,\Delta T)$ in the source with propagation component is approximately constant, it is similar to the nth sensor of a static array response. Second, the observed temporal-delay component in (6) is correctable with $\boldsymbol{A}_c = diag([e^{-j\omega\,0\,\Delta T} \quad \ldots \quad e^{-j\omega\,(N-1)\,\Delta T}])$, a temporal correction factor. Applying the first observation and the temporal correction factor $\boldsymbol{A}_c$ arrives at following OSA expression:

$$\boldsymbol{p}_{OSA}(t) = \boldsymbol{A}_c\boldsymbol{p}(t) = A_s e^{j(\omega t+\psi)} \begin{bmatrix} e^{-j\frac{\omega}{c}r(t+0\,\Delta T)} \\ \vdots \\ e^{-j\frac{\omega}{c}r(t+(N-1)\,\Delta T)} \end{bmatrix}, \tag{7}$$

which has a similar response to a static array.

C. Localization through Beamforming

The localization problem can now be solved in the beamforming formulation in three steps. First, the search space immediately in front of the OSA is constructed using grid points. Next, for each of the grid points in the search space, the spatial spectrum energy is computed. Finally, the energy of the grid space is analyzed, and the point with the highest energy is interpreted as the highest likelihood of the source location.

Concretely, let $\mathcal{R} = \{\boldsymbol{r}_1 \quad \cdots \quad \boldsymbol{r}_L\}$ denote the set that contains the search space pointing to the discrete grid points within the OSA search area in a free field, and $\boldsymbol{v} = (v_x, v_y)$ denote the estimated velocity of the sensor moving along a trajectory. The position of each nth synthetic sensor of the OSA can be approximated by the position of the moving sensor when it is at the middle of each nth frame, i.e., at $\boldsymbol{v}\Delta T\,(n - 0.5)$. Now, the steering vector can be constructed as:

$$\boldsymbol{a}(\boldsymbol{r}_j) = \begin{bmatrix} e^{-j\frac{\omega}{c}\sqrt{(x_j - v_x\,0.5\,\Delta T)^2 + (y_j - v_y\,0.5\,\Delta T)^2}} \\ \vdots \\ e^{-j\frac{\omega}{c}\sqrt{(x_j - v_x\,(N-0.5)\,\Delta T)^2 + (y_j - v_y\,(N-0.5)\,\Delta T)^2}} \end{bmatrix}, \tag{8}$$

where $\boldsymbol{r}_j = (x_j, y_j) \in \mathcal{R}$ is the vector pointing to a discrete point within the OSA immediate vector space, ω is the angular frequency of the source, and c is the speed of propagation in the medium.

Next, to compute the beamformer energy of each grid point, the $N \times N$ covariance matrix of the OSA signal must be constructed. Each element of the covariance matrix represents the correlation of two synthetic sensor signals; it is defined as:

$$\boldsymbol{R}_{OSA} = E\{\boldsymbol{p}_{OSA}(t)\boldsymbol{p}_{OSA}^H(t)\} = \boldsymbol{A}_c\boldsymbol{R}_{pp}\boldsymbol{A}_c^H, \tag{9}$$

where $E\{.\}$ and $(.)^H$ correspond to the expectation and the Hermitian operation, respectively. $\boldsymbol{R}_{pp} = E\{\boldsymbol{p}(t)\boldsymbol{p}^H(t)\}$ is the covariance matrix of the OSA before correction. In practical application, this covariance matrix is unavailable and is estimated with its sample covariance matrix [14]:

$$\widehat{\boldsymbol{R}}_{OSA} = \boldsymbol{A}_c\left\{\frac{1}{\tau}\sum_{t=1}^{\tau}\boldsymbol{p}(t)\boldsymbol{p}^H(t)\right\}\boldsymbol{A}_c^H = \boldsymbol{A}_c\widehat{\boldsymbol{R}}_{pp}\boldsymbol{A}_c^H, \tag{10}$$

where τ is the total number of samples. Finally, the source is localized through finding the argument that maximizes the MUSIC spatial spectrum [2, 3, 15, 16]:

$$\hat{\boldsymbol{r}}_s = arg\,max_{\boldsymbol{r}_j \in \mathcal{R}} \frac{1}{\boldsymbol{a}^H(\boldsymbol{r}_j)\widehat{\boldsymbol{G}}_{OSA}\widehat{\boldsymbol{G}}_{OSA}^H\boldsymbol{a}(\boldsymbol{r}_j)}, \tag{11}$$

where $\widehat{\boldsymbol{G}}_{OSA}\widehat{\boldsymbol{G}}_{OSA}^H$ in (11) is the noise subspace of the sample covariance matrix of the OSA. It is computed after performing the following eigen-decomposing operation on (10), $\widehat{\boldsymbol{R}}_{OSA} = \{\widehat{\boldsymbol{S}}_{OSA}\boldsymbol{\Lambda}_{OSA}\widehat{\boldsymbol{S}}_{OSA}^H + \widehat{\boldsymbol{G}}_{OSA}\boldsymbol{\Gamma}_{OSA}\widehat{\boldsymbol{G}}_{OSA}^H\}$ with $\widehat{\boldsymbol{S}}_{OSA}$ and $\boldsymbol{\Lambda}_{OSA}$ being the signal subspace eigenvectors and eigenvalues,

respectively, and $\widehat{\boldsymbol{G}}_{OSA}$ and $\boldsymbol{\Gamma}_{OSA}$ being the noise subspace eigenvectors and eigenvalues, respectively.

However, because the noise subspace of $\widehat{\boldsymbol{R}}_{OSA}$ is a translated noise subspace of $\widehat{\boldsymbol{R}}_{pp}$ with the temporal correction factor $\boldsymbol{A}_c$, i.e., $\widehat{\boldsymbol{G}}_{OSA} = \boldsymbol{A}_c\widehat{\boldsymbol{G}}_{PP}$, where $\widehat{\boldsymbol{G}}_{PP}$ is computed from the eigen-decomposition of $\widehat{\boldsymbol{R}}_{pp} = \widehat{\boldsymbol{S}}_{PP}\boldsymbol{\Lambda}_{PP}\widehat{\boldsymbol{S}}_{PP}^{\mathrm{H}} + \widehat{\boldsymbol{G}}_{PP}\boldsymbol{\Gamma}_{PP}\widehat{\boldsymbol{G}}_{PP}^{\mathrm{H}}$. Therefore, (11) can also be interpreted as:

$$\hat{\boldsymbol{r}}_s = arg\ max_{\boldsymbol{r}_j\in\mathcal{R}} \frac{1}{\boldsymbol{w}^H(\boldsymbol{r}_j)\widehat{\boldsymbol{G}}_{PP}\widehat{\boldsymbol{G}}_{PP}^H\boldsymbol{w}(\boldsymbol{r}_j)}, \tag{12}$$

where $\boldsymbol{w}(\boldsymbol{r}_j) = \boldsymbol{A}_c^{-1}\boldsymbol{a}(\boldsymbol{r}_j) = \boldsymbol{A}_c^H\boldsymbol{a}(\boldsymbol{r}_j)$, is the weights for OSA localization.

D. Harmonic Signal using Beamformer in Frequency Domain

The monopole model in (1) can naturally be extended to the harmonic signal model by the superposition of the pitch and its $I-1$ harmonic component with an unknown phase shift at each ith pitch to capture the random superposition [12]. Now $s(t)$ can be extended to arrive at:

$$s(t) = \sum_{i=1}^{I} A_{s_i} e^{j(\omega t i + \psi_i)}, \tag{13}$$

where A_{s_i} and ψ_i are the amplitude and phase of the ith order harmonic components. Substituting (13) into (2) arrives at the following expression for the moving sensor recording:

$$p(t) = \sum_{i=1}^{I} A_{s_i} e^{j(\omega t i + \psi_i)}\, e^{-j\frac{\omega}{c}r(t)i} + q(t). \tag{14}$$

Now, the OSA recording for (13) before correction can be constructed by substituting (14) into (4).

Coincidentally, to extend the proposed algorithm to solve for a harmonic signal, it is prudent to transform the OSA in (7) to the frequency domain [17] representation. This is necessary to construct the sample covariance matrix of the OSA to capture all harmonic components. The OSA in the frequency domain can now be denoted as:

$$\tilde{\boldsymbol{p}}(k) = \mathcal{F}\{\boldsymbol{p}(t)\} = [\tilde{p}_1(k) \quad \cdots \quad \tilde{p}_N(k)]^T, \tag{15}$$

where $\mathcal{F}\{.\}$ is the Fourier transform operator along the row of (4). The correlation matrix of each frequency bin in (15) can be defined as:

$$\tilde{\boldsymbol{R}}_{pp}(k) = E\{\tilde{\boldsymbol{p}}(k)\tilde{\boldsymbol{p}}^{\mathrm{H}}(k)\}. \tag{16}$$

The temporal correction factor is also extendable to the frequency representation by means of a similar process with:

$$\tilde{\boldsymbol{A}}_c(k) = diag\left(\begin{bmatrix} e^{-j\omega_{\mathrm{k}}\,0\,\Delta T} \\ \vdots \\ e^{-j\omega_{\mathrm{k}}(N-1)\,\Delta T} \end{bmatrix}\right), \tag{17}$$

where $\omega_k = \frac{2\pi}{K}k$, with K being the total number of frequency bins. Applying (17) onto (15) arrives at the following corrected OSA recording for each frequency bin:

$$\tilde{\boldsymbol{p}}_{OSA}(k) = \tilde{\boldsymbol{A}}_c(k)\tilde{\boldsymbol{p}}(k). \tag{18}$$

Similar to (9), the $N \times N$ covariance matrix of the corrected frequency domain OSA at the kth bin is constructed using:

$$\begin{aligned}\tilde{\boldsymbol{R}}_{OSA}(k) &= E\{\tilde{\boldsymbol{p}}_{OSA}(k)\tilde{\boldsymbol{p}}_{OSA}^{\mathrm{H}}(k)\} \\ &= \tilde{\boldsymbol{A}}_c(k)\tilde{\boldsymbol{R}}_{pp}(k)\boldsymbol{A}_c^H(k).\end{aligned} \tag{19}$$

Finally, the localization of the harmonic source can be achieved by substituting (19) into (12) to arrive at:

$$\hat{\boldsymbol{r}}_s = arg\ max_{\boldsymbol{r}_j\in\mathcal{R}} \sum_{k=1}^{I}\beta(\boldsymbol{r}_j, k), \tag{20}$$

where

$$\beta(\boldsymbol{r}_j, k) = \frac{1}{\tilde{\boldsymbol{w}}^{\mathrm{H}}(\boldsymbol{r}_j, k)\tilde{\boldsymbol{G}}_{PP}(k)\tilde{\boldsymbol{G}}_{PP}^H(k)\tilde{\boldsymbol{w}}(\boldsymbol{r}_j, k)},$$

with the nth element of $\tilde{\boldsymbol{w}}(\boldsymbol{r}_j, k)$:

$$[\tilde{\boldsymbol{w}}(\boldsymbol{r}_j, k)]_n = [\tilde{\boldsymbol{A}}_c(k)]_n[\tilde{\boldsymbol{a}}(\boldsymbol{r}_j, k)]_n.$$

Here, $[\tilde{\boldsymbol{A}}_c(k)]_n$ is the nth diagonal value of (17) and $[\tilde{\boldsymbol{a}}(\boldsymbol{r}_j, k)]_n = e^{-j\frac{\omega_k}{c}\sqrt{(x_j - v_x(n-0.5)\Delta T)^2 + (y_j - v_y(n-0.5)\Delta T)^2}}$ is the nth steering vector of the kth bin. Similar to (12), $\tilde{\boldsymbol{G}}_{PP}(k)\tilde{\boldsymbol{G}}_{PP}^H(k)$ is the noise subspace at ω_k, computed through the eigen-decomposing operation.

Practically, in the localization problem, the frequency ω_k of the source signal is usually unknown. Nonetheless, this is easily overcome by performing a power spectrum analysis of the recorded signal in (14) to estimate the principal frequency content of the harmonic source. The frequency estimation of the source can be further refined using standard numerical optimization to find the frequency that maximizes (20).

III. Numerical Analysis

This section presents numerical simulations to illustrate the validity of the OSA approach established in section II. In the simulation, a moving sensor initially located at the origin of the Cartesian coordinate system is made to move with a velocity of $\boldsymbol{v} = (v_x, v_y) = [1,0]$ m/s in the $+x$ direction and a sampling rate of 25.6 kHz. The acoustic propagation medium is assumed to be air with $c = 343$ m/s. First, the OSA localization performance of (12) to a monopole of $f = 250$ Hz was compared with the Cramer-Rao bound (CRB) of the static array (SA) response [18, 19]. In terms of comparison, both OSA and SA were made to have the same number of sensors and available snapshot for the covariance matrix. The CRB is a theoretical statistical bound of a SA covariance matrix at its given signal-to-noise ratio (SNR). Next, the performance of the OSA to a harmonic source of the same frequency of 250 Hz was evaluated.

Fig. 2 depicts the standard deviation of 500 localization trials of the OSA using (12). Here, the standard deviation is compared with the $\sqrt{\mathrm{CRB}}$ for a source in SA at SNR -20 to 10 dB. The OSA is constructed with $\Delta T = 60$ sec, $N =$

384 synthetic sensors, with each sensor having an inter-sensor spacing of 0.15625 m, and the source located at $\boldsymbol{r}_0 = (30,15)\ m$. Here, perfect knowledge of the signal's frequency is assumed to evaluate only the localization performance.

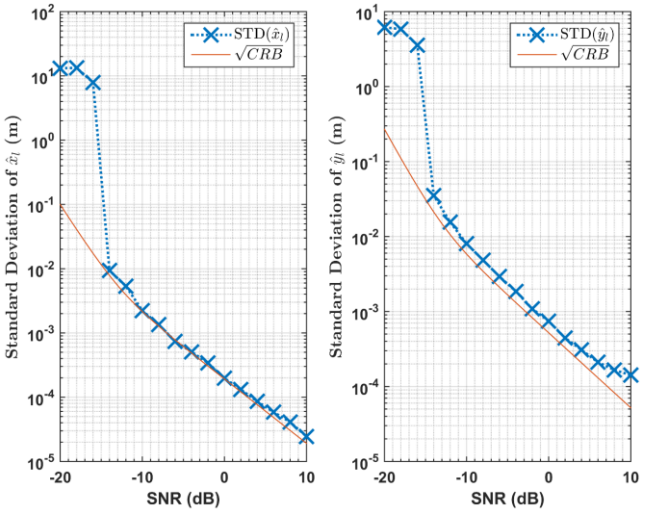

Fig. 2: A comparison plot of the OSA standard deviation to the $\sqrt{CRB}$ of the static array for (left) $\hat{x}_l$ estimation and (right) $\hat{y}_l$ estimation.

The estimation performance of $\hat{x}_l$ and $\hat{y}_l$ of the OSA closely follows the CRB of the SA over a wide range of SNR. The convergence of $\hat{y}_l$ begins at SNR of +8 dB. Nonetheless, poorer performance at higher SNR is expected because of the model approximation error. Finally, the estimation performance of OSA will degrade if the nth synthetic sensor is not modeled at $\hat{\boldsymbol{v}}\Delta T\,(n-0.5)$ because of poorer model approximation.

Fig. 3 depicts the evaluation of (21) using 500 Monte Carlo trials. A harmonic source with $I = 3$ and fundamental frequency of 250 Hz is prepared, each with a variance of one and random phase of $\psi = [-\pi, +\pi]$. The recording duration of the OSA is constructed with $\Delta T = 10$ sec, $N = 20$ synthetic sensor, with each sensor having an inter-sensor spacing of 0.5 m. The signal is located at $\boldsymbol{r}_0 = (4,15)$ m with its SNR varied based on the ratio of signal energy and noise, i.e., $SNR = E\{s(t)\}/E\{q(t)\}$. The only information assumed about the signal is that it is a harmonic source. Therefore, to acquire information, such as the frequencies of the signal, we propose to use the Welch power spectral density (PSD) [20]. The signal frequencies are first estimated using the PSD before applying (20). Because the PSD approach only provides an estimate of the frequencies, numerical optimization is required to determine the true signal frequencies.

The performance of the OSA is compared with the results when the true frequency information is available and the estimation performance when a SA is used. When the estimated frequency is accurate, the performance of the OSA is comparable to that of the SA. In addition, when the signal frequency of the OSA is estimated and optimized, the performance approaches that of an SA at high SNR. This result illustrates that the localization of a harmonic source is robust when a good estimate of the frequency is available.

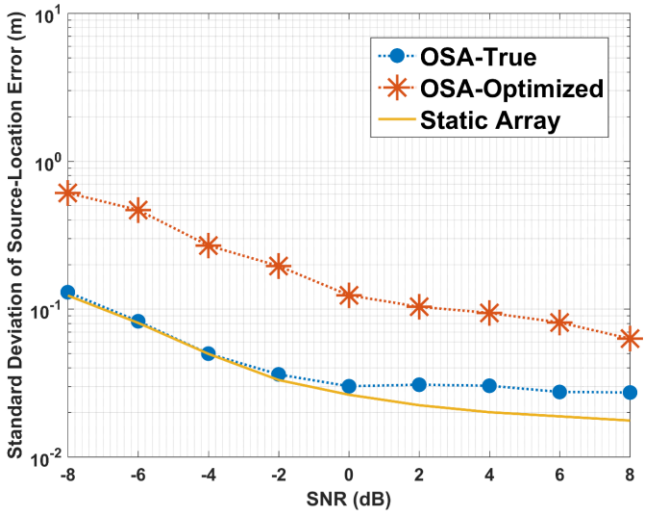

Fig. 3: A comparison between the OSA standard deviation of source-location estimation error, $\|\hat{\boldsymbol{r}}_l - \boldsymbol{r}_0\|$, when the frequencies are known and estimated to the SA standard deviation of source-location estimation error.

IV. Experimental Results

After the simulation, the OSA algorithm was applied to a set of data collected from a driving experiment from [21] as depicted in Fig. 4. The microphone is mounted on top of an electric vehicle (EV) located at $(x, y) = (+6.605, -0.25)$ m. The EV traverses along a linear path at approximately $v = 5.08$ km/hr with a speaker located at $\boldsymbol{r}_0 = (30, 15)$ broadcasting a composite square wave of 250 Hz, 750 Hz, and 1250 Hz. The recording was performed for $\Delta T = 27$ sec at a sampling rate of $F_s = 25.6$ kHz. Using (21), $N = 60$ synthetic sensor was created. As in the harmonic signal simulation, no knowledge of the frequency was assumed. Consequently, the Welch PSD and numerical optimization are used to identify the spectral response before applying (20).

Fig. 4: Experimental setup of the OSA recording using the electric vehicle (EV) with the microphone mounted on top.

Fig. 5 shows the recorded signal and MUSIC spatial spectrum of the OSA model with a beamformer resolution of 0.25 m at the combined spatial spectrum. Although the source was localized with a source-location estimation error, it is attributable to the difficulty of maintaining a constant velocity along the drive-by trajectory [21]. Nonetheless, the results demonstrated that OSA localization of a harmonic source is achievable using a single moving sensor with an approximately known velocity.

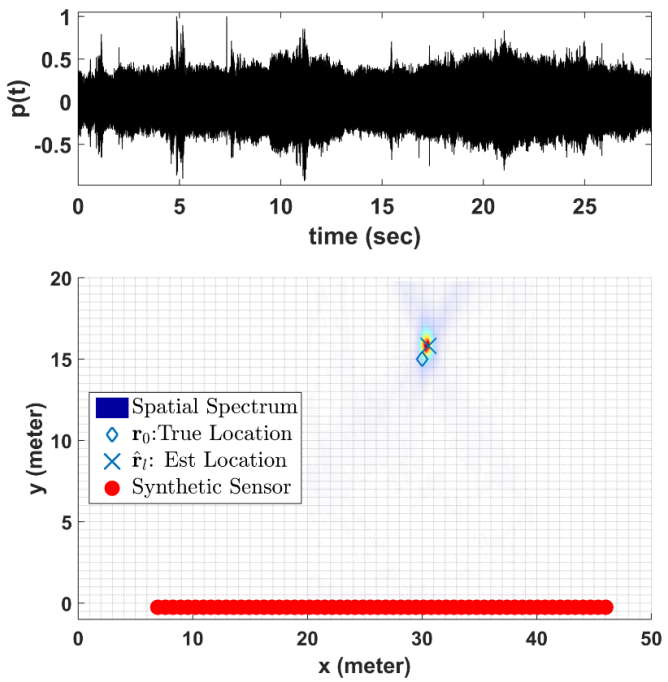

Fig. 5: Recorded signal (top) and MUSIC spatial spectrum (bottom) of the OSA on the drive-by experimental, Combined: $\hat{\boldsymbol{r}}_l = (30.55, 15.8)$.

V. Conclusion

This paper addresses the problems of performing localization when there is insufficient space for sensor placement and demonstrates that harmonic source localization is achievable using the OSA approach based on a single moving sensor of a known piecewise-linear trajectory. The proposed approach consists of three steps. (1) The data are acquired from a single sensor moving along a trajectory with a known velocity $\boldsymbol{v}$ while observing the signal. (2) The data are then preprocessed to decompose the signal into frames before synchronizing the frames through the application of a temporal correction factor. (3) Finally, conventional beamforming is applied for source localization. The numerical simulation conducted and experimental verification shows that the proposed technique can be applied to localize a harmonic source using a single moving sensor. Essentially, this work advances the framework of using one sensor for DOA estimation beyond a circular trajectory.

Acknowledgment

The authors would like to thank C. Tuna, S. Zhao, T. N. T. Nguyen, and D. L. Jones with Advanced Digital Sciences Center Illinois at Singapore Pte Ltd, 1 Fusionopolis Way, Singapore 138632, for providing the experimental data. The authors would also wish to thank Freeman Hill, Yinghui Lu, Srinivasan Jagannathan, and the management of Halliburton for their help and permission to publish this paper.

References

[1] D. H. Johnson and D. E. Dudgeon, Array Signal Processing: Concepts and Techniques: Prentice Hall, 1993.

[2] J. Capon, "High-resolution frequency-wavenumber spectrum analysis," Proceedings of the IEEE, vol. 57, pp. 1408-1418, 1969.

[3] R. O. Schmidt, "Multiple emitter location and signal parameter estimation," Antennas and Propagation, IEEE Transactions on, vol. 34, pp. 276-280, 1986.

[4] F. Gao and A. B. Gershman, "A generalized ESPRIT approach to direction-of-arrival estimation," IEEE Signal Processing Letters, vol. 12, pp. 254-257, 2005.

[5] K. Harmanci, J. Tabrikian, and J. L. Krolik, "Relationships between adaptive minimum variance beamforming and optimal source localization," IEEE Transactions on Signal Processing, vol. 48, pp. 1-12, 2000.

[6] M. P. Hayes and P. T. Gough, "Synthetic aperture sonar: a review of current status," IEEE Journal of Oceanic Engineering, vol. 34, pp. 207-224, 2009.

[7] S. Stergiopoulos and E. J. Sullivan, "Extended towed array processing by an overlap correlator," The Journal of the Acoustical Society of America, vol. 86, pp. 158-171, 1989.

[8] Z. Lei, K. Yang, R. Duan, and P. Xiao, "Localization of low-frequency coherent sound sources with compressive beamforming-based passive synthetic aperture," The Journal of the Acoustical Society of America, vol. 137, pp. EL255-EL260, 2015.

[9] X. Da, N. Tingting, H. Jianguo, and G. Hongya, "Source localization in near-field using a moving array," in Military Communications Conference, 2009. MILCOM 2009. IEEE, 2009, pp. 1-5.

[10] A. Cigada, M. Lurati, F. Ripamonti, and M. Vanali, "Moving microphone arrays to reduce spatial aliasing in the beamforming technique: theoretical background and numerical investigation," The Journal of the Acoustical Society of America, vol. 124, pp. 3648-3658, 2008.

[11] M. Kishida and Y. Hioka, "Circularly moving sensor for use of modulation effect," in Sensing Technology (ICST), 2013 Seventh International Conference on, 2013, pp. 242-246.

[12] Y. Hioka and M. Kishida, "Direction of arrival estimation of harmonic signal using single moving sensor," in 2014 IEEE 8th Sensor Array and Multichannel Signal Processing Workshop (SAM), 2014, pp. 1-4.

[13] W. K. Ma, T. H. Hsieh, and C. Y. Chi, "DOA Estimation of Quasi-Stationary Signals With Less Sensors Than Sources and Unknown Spatial Noise Covariance: A Khatri-Rao Subspace Approach," IEEE Transactions on Signal Processing, vol. 58, pp. 2168-2180, 2010.

[14] I. S. Reed, J. D. Mallett, and L. E. Brennan, "Rapid Convergence Rate in Adaptive Arrays," Aerospace and Electronic Systems, IEEE Transactions on Aerospace and Electronic Systems, vol. AES-10, pp. 853-863, 1974.

[15] P. Stoica and R. L. Moses, Spectral Analysis of Signals: Pearson Prentice Hall, 2005.

[16] P. Stoica and R. L. Moses, Introduction to Spectral Analysis vol. 1: Prentice-Hall Upper Saddle River, New Jersey,1997.

[17] H. L. Van Trees, Detection, Estimation, and Modulation Theory, Optimum Array Processing: John Wiley & Sons, 2004.

[18] E. Grosicki, K. Abed-Meraim, and H. Yingbo, "A weighted linear prediction method for near-field source localization," IEEE Transactions on Signal Processing, vol. 53, pp. 3651-3660, 2005.

[19] P. Stoica, E. G. Larsson, and A. B. Gershman, "The stochastic CRB for array processing: a textbook derivation," Signal Processing Letters, IEEE, vol. 8, pp. 148-150, 2001.

[20] J. G. Proakis and D. G. Manolakis, Digital Signal Processing: Pearson Prentice Hall, 2007.

[21] C. Tuna, S. Zhao, T. N. T. Nguyen, and D. L. Jones, "Drive-by large-region acoustic noise-source mapping via sparse beamforming tomography," The Journal of the Acoustical Society of America, vol. 140, pp. 2530-2541, 2016.